



UNIVERSIDADE ESTADUAL DE CAMPINAS  
SISTEMA DE BIBLIOTECAS DA UNICAMP  
REPOSITÓRIO DA PRODUÇÃO CIENTÍFICA E INTELLECTUAL DA UNICAMP

**Versão do arquivo anexado / Version of attached file:**

Versão do Editor / Published Version

**Mais informações no site da editora / Further information on publisher's website:**

<https://jcs.biologists.org/content/128/1/27.short>

**DOI: 10.1242/jcs.150573**

**Direitos autorais / Publisher's copyright statement:**

©2014 by The Company of Biologists. All rights reserved.

DIRETORIA DE TRATAMENTO DA INFORMAÇÃO

Cidade Universitária Zeferino Vaz Barão Geraldo

CEP 13083-970 – Campinas SP

Fone: (19) 3521-6493

<http://www.repositorio.unicamp.br>

## SHORT REPORT

# The exocyst is required for trypanosome invasion and the repair of mechanical plasma membrane wounds

Maria Cecilia Fernandes, Matthias Corrotte, Danilo C. Miguel\*, Christina Tam<sup>†,§</sup> and Norma W. Andrews<sup>¶</sup>

## ABSTRACT

The process of host cell invasion by *Trypanosoma cruzi* shares mechanistic elements with plasma membrane injury and repair. Both processes require Ca<sup>2+</sup>-triggered exocytosis of lysosomes, exocytosis of acid sphingomyelinase and formation of ceramide-enriched endocytic compartments. *T. cruzi* invades at peripheral sites, suggesting a need for spatial regulation of membrane traffic. Here, we show that Exo70 and Sec8 (also known as EXOC7 and EXOC4, respectively), components of the exocyst complex, accumulate in nascent *T. cruzi* vacuoles and at sites of mechanical wounding. Exo70 or Sec8 depletion inhibits *T. cruzi* invasion and Ca<sup>2+</sup>-dependent resealing of mechanical wounds, but does not affect the repair of smaller lesions caused by pore-forming toxins. Thus, *T. cruzi* invasion and mechanical lesion repair share a unique requirement for the exocyst, consistent with a dependence on targeted membrane delivery.

**KEY WORDS:** Trypanosome, Infection, Resealing

## INTRODUCTION

The protozoan parasite *Trypanosoma cruzi* utilizes the plasma membrane repair machinery for host cell invasion (Fernandes et al., 2011). This machinery includes proteins involved in Ca<sup>2+</sup>-dependent lysosomal exocytosis (Tardieux et al., 1992) and a rapid form of endocytosis triggered by the release of lysosomal acid sphingomyelinase (ASM) (Fernandes et al., 2011; Idone et al., 2008; Tam et al., 2010). Because *T. cruzi* enters cells in a polarized fashion at the cell periphery, through a process that requires exocytosis (Reddy et al., 2001), we investigated the involvement of the exocyst, a conserved octameric protein complex composed of Sec3, Sec5, Sec6, Sec8, Sec10, Sec15, Exo70 and Exo84 (also known as EXOC1–EXOC8) (Guo et al., 2000; Heider and Munson, 2012; TerBush et al., 1996; TerBush and Novick, 1995), which spatially targets vesicles to the plasma membrane (Boyd et al., 2004; He and Guo, 2009; Moskalenko et al., 2003; Liu and Guo, 2012.).

## RESULTS AND DISCUSSION

### The exocyst complex is recruited to vacuoles containing recently internalized *T. cruzi* and is required for efficient invasion

Exo70 and Sec8 were observed to be associated with sites of contact of extracellular *T. cruzi* with the host plasma membrane, as identified

by the staining of exposed parasite portions with antibodies specific to *T. cruzi*. Recruitment of Exo70 and Sec8 was markedly stronger around internalized parasite regions (Fig. 1A,B).

The exocyst complex regulates the exocytosis of post-Golgi vesicles (Guo et al., 1999; Guo et al., 2000; He et al., 2007; Hsu et al., 2004; Liu et al., 2007), so we investigated whether post-Golgi vesicles contribute to the formation of the *T. cruzi* parasitophorous vacuole. HeLa cells were transduced with a construct encoding temperature-sensitive VSVG-ts045–YFP before infection. At the restrictive temperature (39°C) VSVG-ts045–YFP is misfolded and retained in the endoplasmic reticulum. Shifting cells to 37°C allows correct folding and trafficking of the protein through the Golgi to the plasma membrane. Cells were infected with *T. cruzi* at increasing periods after shifting to 37°C, fixed and imaged by confocal microscopy. Recently internalized parasites (inaccessible to anti-*T. cruzi* antibodies) were not associated with VSVG-ts045–YFP at any time-point (Fig. 1C), indicating that Golgi-derived membrane traffic is not directed to nascent parasitophorous vacuoles. This new finding complements earlier studies suggesting that intracellular membrane that is recruited to form *T. cruzi*-containing vacuoles is largely derived from the endosomal or lysosomal compartment (Fernandes et al., 2011; Tardieux et al., 1992; Woolsey et al., 2003).

RNA interference (RNAi)-mediated depletion of Exo70 or Sec8 caused a significant decrease in the number of intracellular parasites when compared with that of cells treated with control siRNA (Fig. 1D,E). Collectively, these results suggest that recruitment of the exocyst complex to nascent parasitophorous vacuoles might regulate localized membrane addition at specific peripheral sites associated with *T. cruzi* entry.

### Generalized Ca<sup>2+</sup>-dependent exocytosis of lysosomes is not inhibited in cells depleted in the exocyst component Exo70

The unique invasion process utilized by *T. cruzi* requires exocytic and endocytic events driven by cytosolic Ca<sup>2+</sup> transients, which are triggered when trypomastigotes initiate contact with host cells (Woolsey et al., 2003; Fernandes et al., 2011). Ca<sup>2+</sup> signaling promotes recruitment and fusion of host lysosomes at the invasion site, a process involved in *T. cruzi* invasion of host cells (Tardieux et al., 1992). Thus, our results suggested that the exocyst might promote exocytosis of lysosomes at the invasion site, facilitating parasite invasion. To determine whether the exocyst was involved in generalized lysosomal exocytosis triggered by intracellular Ca<sup>2+</sup> transients, we measured exocytosis of the lysosomal enzyme β-hexosaminidase in cells depleted of Exo70 and exposed to Ca<sup>2+</sup> influx by permeabilization with the pore-forming toxin SLO (Fig. 2A), scraping from the substrate (Fig. 2B) or treatment with the Ca<sup>2+</sup> ionophore ionomycin (not shown). Under all three conditions, Exo70-deficient cells showed comparable or higher levels of β-hexosaminidase secretion in response to Ca<sup>2+</sup> influx, as

Department of Cell Biology and Molecular Genetics, University of Maryland, College Park, MD 20742-5815, USA.

\*Present address: Department of Animal Biology, Institute of Biology, University of Campinas-UNICAMP, 13083-862 Campinas, SP, Brazil. †Present address: Howard Taylor Ricketts Laboratory, Argonne National Laboratory, Lemont, IL 60439, USA. §Present address: Department of Microbiology, University of Chicago, Chicago, IL 60637, USA.

¶Author for correspondence (andrewsn@umd.edu)

Received 24 January 2014; Accepted 22 October 2014

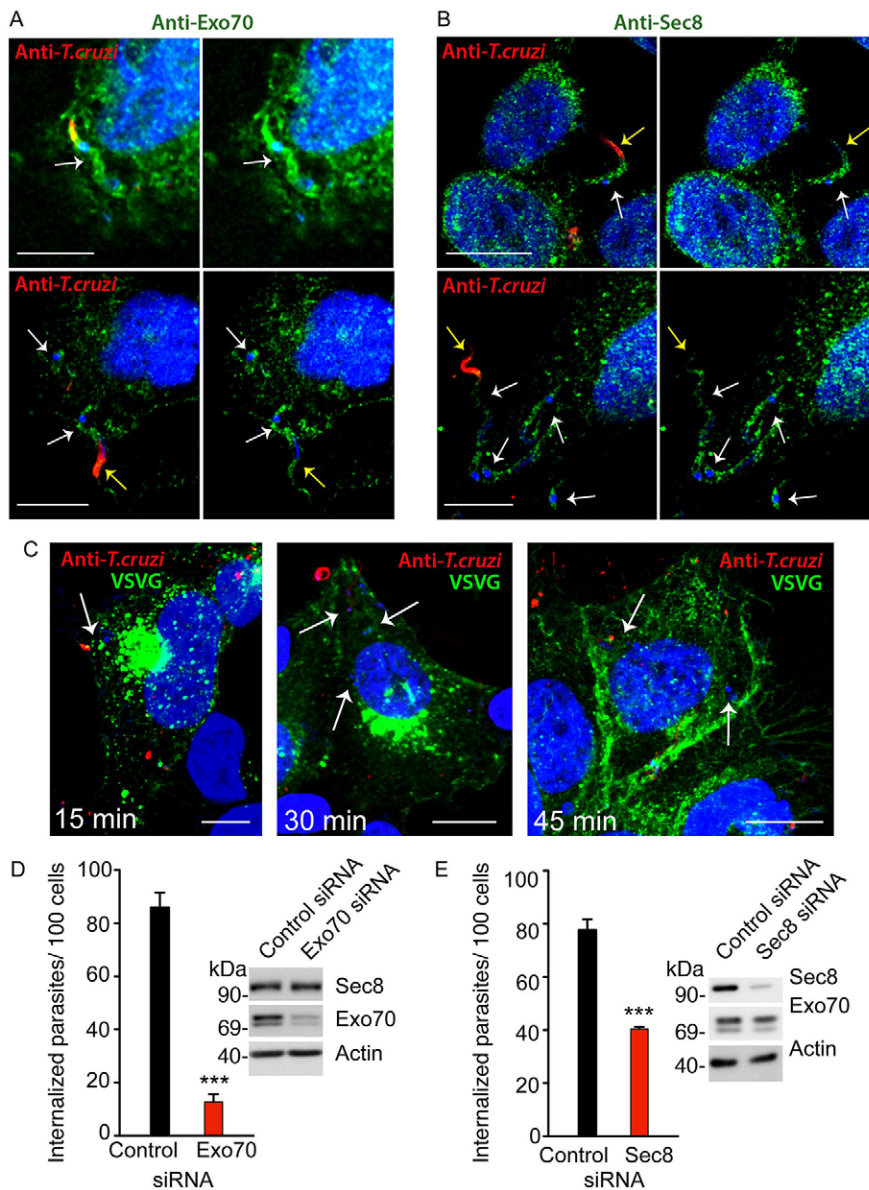


**Fig. 1. Exo70 and Sec8 are recruited to *T. cruzi* parasitophorous vacuoles and are required for host cell invasion.** (A,B) Confocal images of HeLa cells infected with *T. cruzi* trypomastigotes for 30 min and stained with anti-*T. cruzi* antibodies (red) and mAbs against Exo70 (A) or Sec8 (B) (green). Host and parasite DNA were stained with DAPI (blue). White arrows indicate fully internalized trypomastigotes; yellow arrows indicate extracellular parasite regions accessible to anti-*T. cruzi* antibodies before permeabilization. Scale bars: 10  $\mu$ m. The images on the right of each panel show only anti-Exo70 or Sec8 staining and DAPI. (C) Confocal images of HeLa cells expressing VSVG-ts045-YFP (green) and shifted from 39°C to 37°C for the indicated periods, exposed to trypomastigotes for 10 min and stained with anti-*T. cruzi* (red) and DAPI (blue). White arrows indicate internalized parasites. Scale bars: 10  $\mu$ m. (D,E) Quantification of intracellular parasites in HeLa cells transfected for 72 h with control, Exo70-specific (D) or Sec8-specific (E) siRNA and infected for 1 h. The data correspond to the mean of triplicates ( $\pm$ s.d.); \*\*\* $P \leq 0.0004$  (between cells treated with control and Exo70- or Sec8-specific siRNA; Student's *t*-test). Insets show western blots indicating that ~80% knockdown was achieved for each protein.

compared with controls. This result suggests that the inhibition of *T. cruzi* invasion in cells depleted in Exo70 and Sec8 is not a consequence of an intrinsic defect in  $Ca^{2+}$ -triggered lysosomal exocytosis. However, these results do not rule out the possibility that the exocyst complex is required for the highly localized lysosome recruitment and fusion events observed at *T. cruzi* invasion sites (Tardieux et al., 1992). The increase in generalized  $Ca^{2+}$ -dependent lysosomal exocytosis in Exo70-depleted cells might be related to changes in the cortical actin cytoskeleton, consistent with the demonstration that Exo70 acts as a kinetic activator of Arp2/3, promoting actin filament nucleation and branching (Liu et al., 2012).

#### The exocyst is required for the repair of mechanical wounds but not for plasma membrane resealing after injury with the pore-forming toxin SLO

Given that the exocyst plays a role in spatially targeting vesicles to the plasma membrane (Heider and Munson, 2012), we also investigated whether the depletion of exocyst components had a

differential effect on the repair of polarized (mechanical) and non-polarized (pore-forming toxin SLO) wounds. After SLO exposure, cells were incubated under conditions that were permissive ( $Ca^{2+}$ ) or non-permissive (no  $Ca^{2+}$ ) for plasma membrane repair, and exposed to the membrane-impermeant dye propidium iodide. Cells treated with control or Exo70-specific siRNA were equally capable of resealing their plasma membrane after SLO permeabilization in the presence of  $Ca^{2+}$ , as indicated by the block in uptake (Fig. 2C, right panels). As expected, without  $Ca^{2+}$ , permeabilized cells did not reseal, allowing propidium iodide influx (Fig. 2C, left panels). Flow cytometric quantification of propidium-iodide-positive cells confirmed that depletion of Exo70 (Fig. 2D) or Sec8 (Fig. 2E) did not affect the ability of the cells to repair their plasma membrane after permeabilization with the toxin SLO, which binds to cholesterol and forms stable transmembrane pores with an external diameter of ~30 nm (Tveten, 2005).

In contrast, Exo70-depleted cells that were mechanically wounded by scraping from the substrate were not able to block

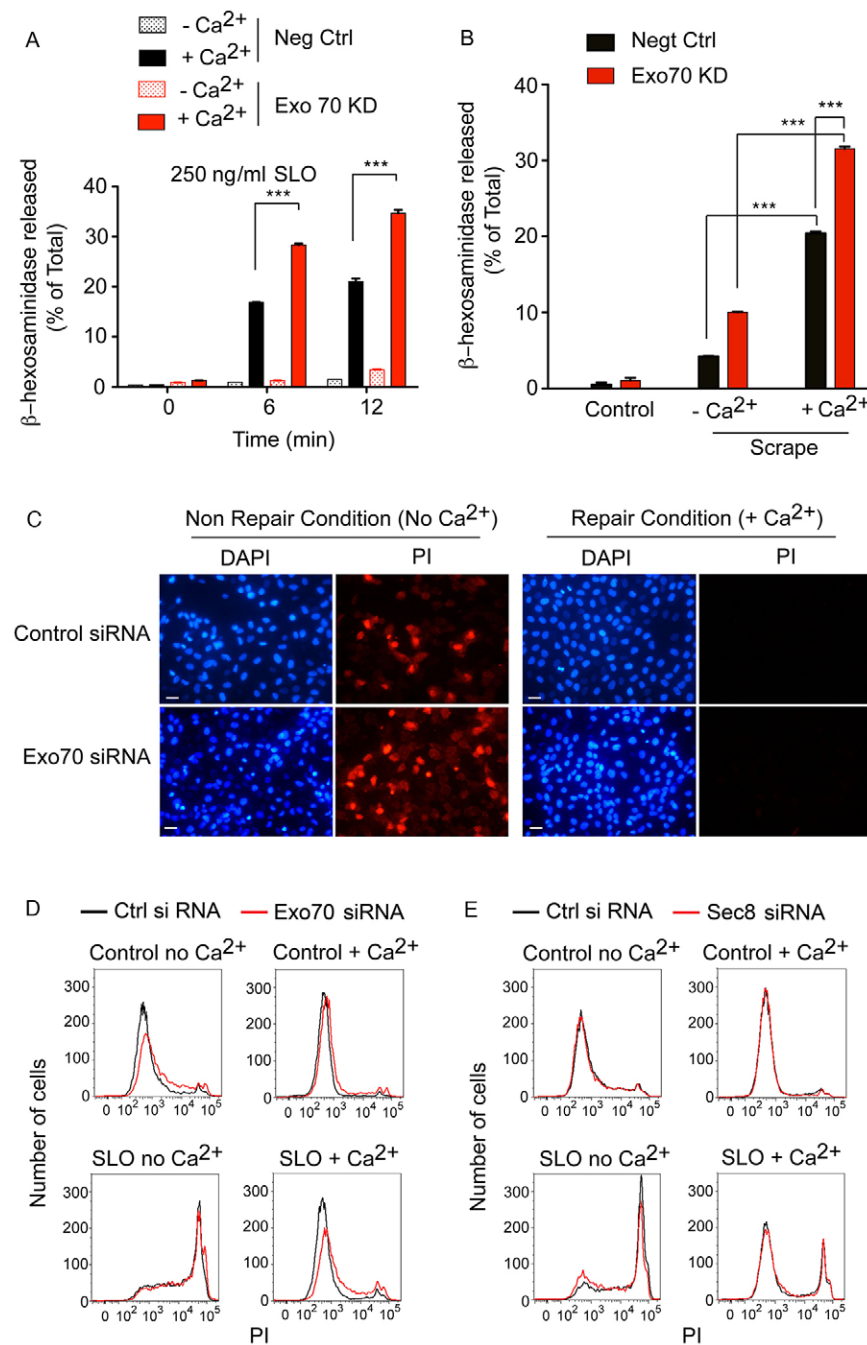


**Fig. 2. Generalized Ca<sup>2+</sup>-dependent lysosomal exocytosis and Ca<sup>2+</sup>-dependent resealing of cells permeabilized with SLO are not impaired in cells deficient in exocyst components.** NRK cells were transfected with control (Neg Ctrl) or Exo70-specific (Exo70 KD) siRNA, and the secretion of  $\beta$ -hexosaminidase was measured in the supernatant after (A) treatment with the indicated concentration of SLO or (B) scraping from the dish. The data correspond to the mean of triplicates ( $\pm$ s.d.); \*\*\* $P \leq 0.0002$  (Student's  $t$ -test). (C) HeLa cells transfected with control or Exo70-specific siRNA were treated with 300 ng/ml SLO for 5 min on ice and shifted to 37°C to induce pore formation with or without Ca<sup>2+</sup> for 3 min. After incubation with propidium iodide (PI) for 1 min, cells were fixed, stained with DAPI and imaged. Scale bars: 20  $\mu$ m. (D) Flow cytometric analysis of HeLa cells transfected with control (black) or Exo70-specific (red) siRNA, before (upper panels) or after (lower panels) SLO permeabilization in the presence or absence of Ca<sup>2+</sup>. (E) Flow cytometric analysis of HeLa cells transfected with control (black) or Sec8-specific (red) siRNA, before (upper panels) or after (lower panels) SLO permeabilization in the presence or absence of Ca<sup>2+</sup>.

propidium iodide influx in the presence of Ca<sup>2+</sup>, reflecting a defect in plasma membrane repair (Fig. 3A). Flow cytometric quantification of propidium-iodide-positive cells after scraping (Fig. 3B,C) confirmed this result, showing that silencing of Exo70 (Fig. 3B, lower right panel) or Sec8 (Fig. 3C, lower right panel) resulted in a strong defect in Ca<sup>2+</sup>-dependent plasma membrane repair. To examine the effect of mechanical wounding on the distribution of Exo70, we injured cells by contact with glass beads in the presence or absence of extracellular Ca<sup>2+</sup>, and performed immunofluorescence with antibodies against endogenous Exo70. Wounded cells were identified by intracellular staining with a membrane-impermeant fluorescent dextran added to the medium during wounding. In non-wounded cells, Exo70 showed a typical punctate intracellular pattern, with

minimal association with the plasma membrane, and the presence or absence of Ca<sup>2+</sup> had no impact on this steady-state distribution (Fig. 4A–D). However, when the cells were wounded with glass beads for 30 s or 3 min, Exo70 was redistributed to the plasma membrane (Fig. 4E–M).

Collectively, our results show that the exocyst tethering complex is recruited to sites of mechanical wounding and of *T. cruzi* entry, and that this is required for plasma membrane repair and for cell invasion by the parasites. This suggests that the exocyst, which has been previously linked to constitutive secretion, can also regulate Ca<sup>2+</sup>-dependent membrane trafficking events necessary for plasma membrane remodeling. Interestingly, previous studies implicated the exocyst in neurite outgrowth (Murthy et al., 2003), a polarized process that involves

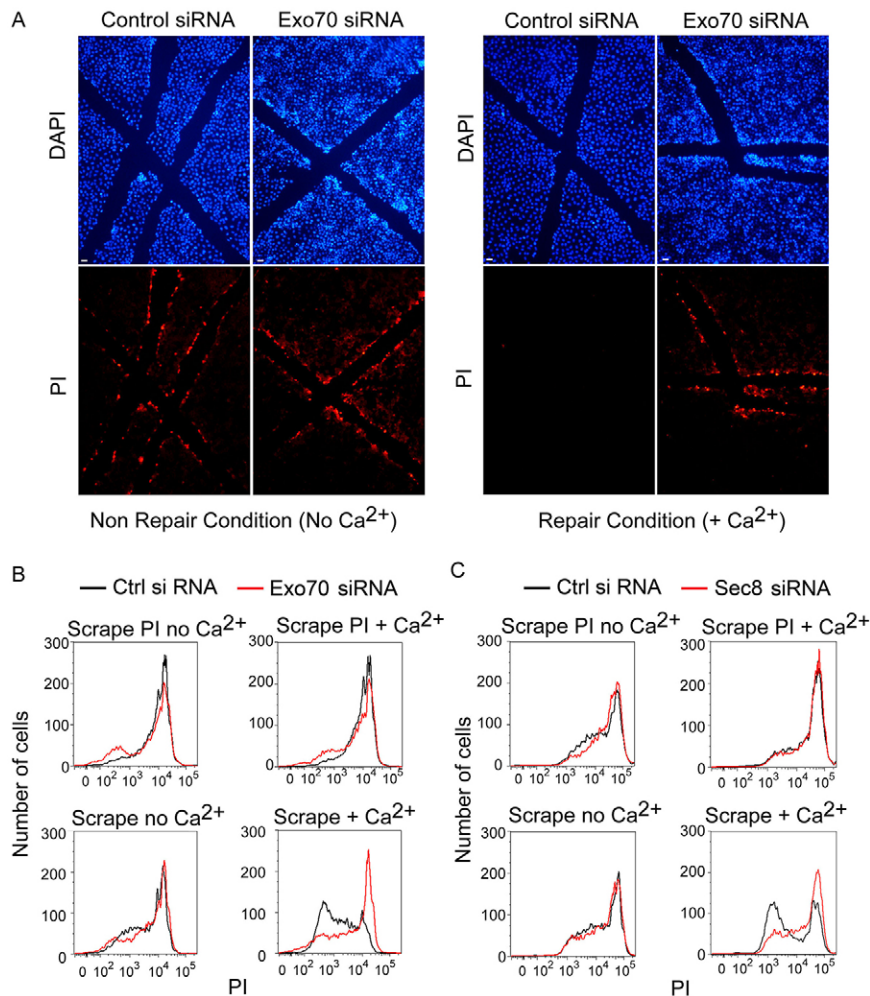


**Fig. 3. Cells depleted of Exo70 or Sec8 fail to repair mechanical wounds.** (A) NRK cell monolayers transfected with control or Exo70-specific siRNA were scratched with a needle in the presence or absence of  $\text{Ca}^{2+}$  and, after 3 min at  $37^\circ\text{C}$ , were incubated with propidium iodide (PI), fixed, stained with DAPI and imaged. Scale bars: 20  $\mu\text{m}$ . (B) Flow cytometric analysis of scraped HeLa cells transfected with control (Ctrl, black) or Exo70-specific (red) siRNA in the presence or absence of  $\text{Ca}^{2+}$ . Upper panels show cells scraped in the presence of propidium iodide; high fluorescence levels indicate that the whole cell population was wounded. Lower panels show cells incubated with propidium iodide 3 min after wounding; reduced propidium iodide staining reflects repair levels. (C) Flow cytometric analysis of scraped HeLa cells transfected with control (black) or Sec8-specific (red) siRNA in the presence or absence of  $\text{Ca}^{2+}$ . Upper panels show cells scraped in the presence of propidium iodide. Lower panels show incubation with propidium iodide at 3 min after wounding.

the lysosomal SNARE TI-VAMP (also known as VAMP7) (Martinez-Arca et al., 2000) and the lysosomal  $\text{Ca}^{2+}$  sensor synaptotagmin 7 (Arantes and Andrews, 2006). Thus, the role of the exocyst in *T. cruzi* invasion and in resealing of mechanical wounds might be attributed to a need for highly localized, spatially regulated lysosomal exocytosis, similar to the process of neurite outgrowth. We cannot rule out, however, that non-lysosomal sources of intracellular membrane contribute to these processes in an exocyst-dependent manner. Regardless of the origin of the exocyst-regulated secretory vesicles, our findings reveal functional differences between the repair of large localized mechanical wounds and smaller homogeneously distributed pores generated by the cholesterol-binding toxin SLO. Thus, the resealing of mechanical wounds and *T. cruzi* invasion might both require polarized exocyst-mediated membrane delivery because they involve events that are restricted to specific plasma membrane sites.

## MATERIALS AND METHODS

### Host cells and parasites

HeLa CCL-2.1 and normal rat kidney (NRK) cells were grown in Dulbecco's modified Eagle's medium (DMEM) (Gibco) supplemented with 10% FBS at  $37^\circ\text{C}$  under 5%  $\text{CO}_2$ . Trypomastigotes from the *Trypanosoma cruzi* Y strain were obtained from the supernatant of infected monolayers of LLC-MK<sub>2</sub> cells as described previously (Andrews et al., 1987).

### Invasion assays and immunofluorescence

$1.8 \times 10^5$  cells were plated in 35-mm wells on glass coverslips 24 h before experiments and incubated with  $1 \times 10^8$  *T. cruzi* trypomastigotes in 2 ml of DMEM (containing 2% FBS) per well for various periods of time at  $37^\circ\text{C}$ , washed five times with PBS to remove extracellular parasites, fixed with 4% paraformaldehyde (PFA) in PBS for 15 min and processed for inside/outside immunofluorescence (Tardieux et al., 1992). Intracellular parasites were quantified in  $\sim 300$  host cells per coverslip in triplicate, by using a Nikon E200 microscope with a  $100\times$  NA 1.3 oil objective. For the staining of exocyst components, cells were permeabilized with 0.2% Triton X-100 for 5 min and incubated with mouse monoclonal antibodies (mAb) against Exo70 (Zuo et al., 2006) or Sec8 (Liu et al., 2009) (provided by Dr Wei Guo, University of Pennsylvania, PA) for 1 h, followed by incubation with anti-mouse-IgG secondary antibodies conjugated to Alexa Fluor 488 (Invitrogen). Images were acquired on a laser-scanning confocal Leica SPX5 with a  $63\times$  NA 1.4 oil objective. DNA in all samples was stained with 10  $\mu\text{M}$  DAPI (Sigma).

### Resealing and exocytosis assays

Cell monolayers (at 60% confluence) were washed three times at  $4^\circ\text{C}$  with  $\text{Ca}^{2+}$ -free DMEM (containing  $\text{Mg}^{2+}$  and 10 mM EGTA) and treated with histidine-tagged SLO (R. Tweeten, University of Oklahoma, OK) in  $\text{Ca}^{2+}$ -free DMEM for 5 min at  $4^\circ\text{C}$ . Pore formation was triggered by replacing the medium with  $37^\circ\text{C}$  DMEM with or without 1.8 mM  $\text{Ca}^{2+}$ . After 3 min, cells were stained with 50  $\mu\text{g}/\text{ml}$  propidium iodide (Sigma) for 1 min. For flow cytometry assays,  $1 \times 10^6$  trypsinized cells were incubated with SLO for 5 min at  $4^\circ\text{C}$  in 250  $\mu\text{l}$  of  $\text{Ca}^{2+}$ -free DMEM, followed by incubation at  $37^\circ\text{C}$  in DMEM with or without  $\text{Ca}^{2+}$  and

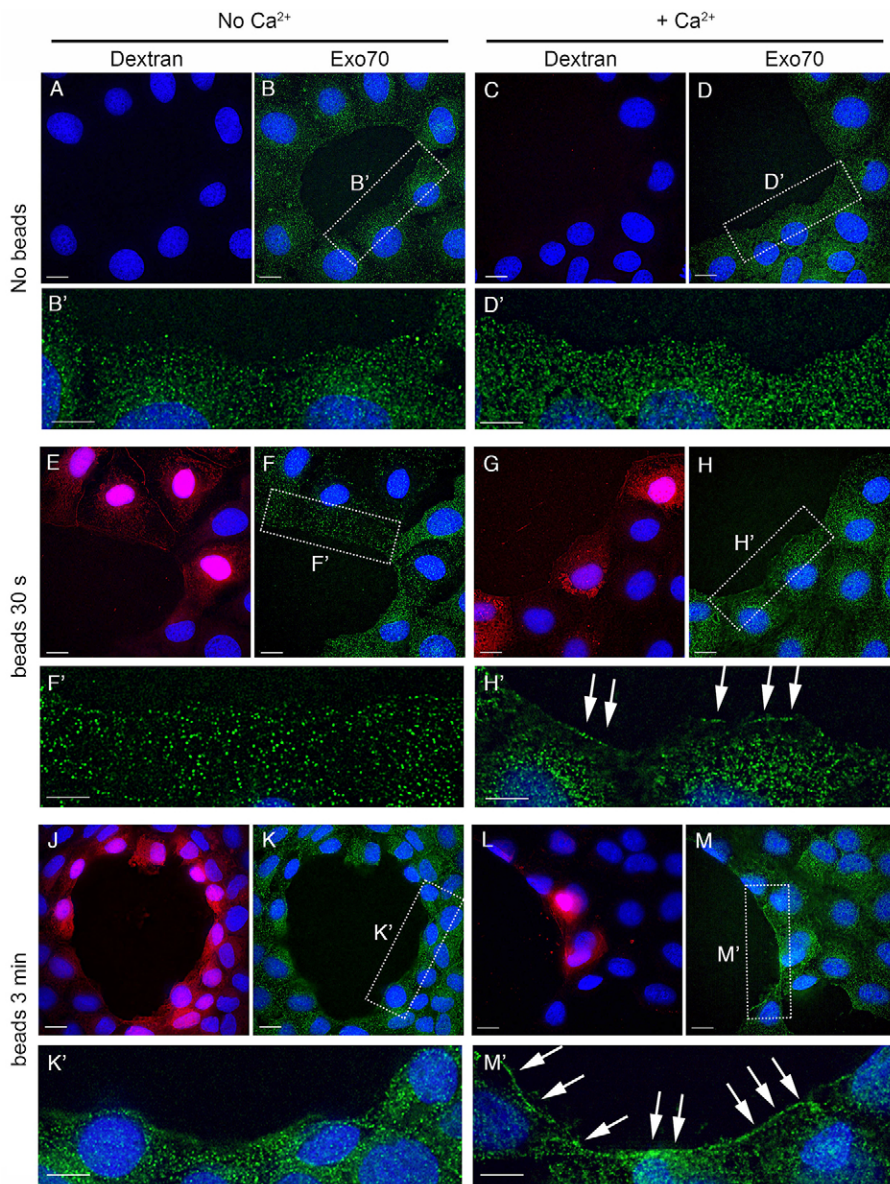


**Fig. 4. Exo70 is recruited to the plasma membrane at sites of mechanical wounding.** NRK cells were either wounded with glass beads or left unwounded in the presence of fluorescent dextran (red), fixed, stained with DAPI (blue) and anti-Exo70 antibodies (green), and imaged. (A,B) Non-wounded cells incubated in  $\text{Ca}^{2+}$ -free medium. (B') Higher magnification of the region outlined in B. (C,D) Non-wounded cells incubated in  $\text{Ca}^{2+}$ -containing medium. (D') Higher magnification of the region outlined in D. (E,F) Cells wounded for 30 s in  $\text{Ca}^{2+}$ -free medium. (F') Higher magnification of the region outlined in F. (G,H) Cells wounded for 30 s in  $\text{Ca}^{2+}$ -containing medium. (H') Higher magnification of the region outlined in H. (J,K) Cells wounded for 3 min in  $\text{Ca}^{2+}$ -free medium. (K') Higher magnification of the region outlined in K. (L,M) Cells wounded for 3 min in  $\text{Ca}^{2+}$ -containing medium. (M') Higher magnification of the region outlined in M. Scale bars: 10  $\mu\text{m}$ . The arrows in H' and M' point to Exo70 relocation to the plasma membrane of cells wounded in the presence of  $\text{Ca}^{2+}$  (identified by red dextran staining).

propidium iodide for 4 min. For scrape assays, cells were removed from the dish at 37°C with a rubber policeman (BD Biosciences). Propidium iodide was added during scraping or after 4 min at 37°C in the presence or absence of  $\text{Ca}^{2+}$ . Flow cytometry data from ~10,000 cells (FACSCanto, BD Biosciences) were analyzed using FlowJo 6.3 software (Tree Star, Inc.). For scratch assays, monolayers attached to coverslips were scratched with a needle in DMEM with or without  $\text{Ca}^{2+}$ , incubated for 3 min at 37°C, stained for 1 min with propidium iodide and DAPI, and imaged.  $\beta$ -hexosaminidase secretion assays were performed as described previously (Rodríguez et al., 1997).

#### Wounding with glass beads

NRK cells were cultured on glass coverslips to confluency incubated in 500  $\mu\text{l}$  of DMEM with or without  $\text{Ca}^{2+}$  at 37°C before the medium was exchanged for 500  $\mu\text{l}$  of DMEM with or without  $\text{Ca}^{2+}$  containing 5 mg/ml Texas-Red-dextran (molecular mass of 10,000 Da, lysine fixable; Invitrogen) and cells were mechanically wounded using 500- $\mu\text{m}$  acid-washed glass beads (Sigma) sprinkled (0.05 g per coverslip) from a 1-ml conical tube held 1 cm above the well. Cells were rocked three times and incubated in DMEM with or without  $\text{Ca}^{2+}$  or dextran for various time-points, washed in ice-cold PBS without  $\text{Ca}^{2+}$  and fixed in 4% PFA.

Following immunostaining for Exo70, cells were imaged using a Deltavision Elite deconvolution microscope equipped with an NA 1.42 60 $\times$  objective.

#### RNAi and western blotting

HeLa cells ( $1.4 \times 10^5$ ) in 35-mm wells were transfected with Lipofectamine and 160 pmol of stealth siRNA duplexes according to the manufacturer's instructions (Invitrogen). The duplexes used were control (medium GC content; Invitrogen), 5'-AUAGUGAGAG-GUAUCAAGG-3' (targeting human Sec8), 5'-UCGCAGAGAAGAA-UCUACCGUGUU-3' (targeting human Exo70), 5'-GGCUAAAGG-UGACUGACUA-3' (targeting rat Exo70) or 5'-AUUCCUUGAUGC-CACUCA-3' (targeting rat Sec8). Cells were used for *T. cruzi* invasion or plasma membrane repair assays at 72 h post-transfection. Western blotting for Exo70 or Sec8 was performed on cell lysates that were separated by SDS-PAGE, transferred to nitrocellulose and incubated with mouse anti-Exo70 or mouse anti-Sec8 antibodies.

#### VSVG-YFP trafficking assay

HeLa cells transduced with adenovirus encoding VSVG-ts045-YFP as described previously (Toomre et al., 2000) were placed at 39°C

overnight, shifted to 37°C for 15, 30, 45 and 60 min, exposed to trypomastigotes for 10 min, fixed and processed for the quantification of intracellular parasites.

#### Acknowledgements

We thank Dr D. Toomre (Yale University) for the VSVG construct, Dr W. Guo (University of Pennsylvania) for antibodies and A. Beaven and K. Class (University of Maryland) for assistance with confocal microscopy and flow cytometry, respectively.

#### Competing interests

The authors declare no competing interests.

#### Author contributions

M.C.F. and N.W.A. designed the project; M.C.F., D.C.M. and C.T. performed the parasite invasion, exocytosis and PM repair experiments; M.C. performed the glass bead wounding experiments; M.C.F. and N.W.A. wrote the paper.

#### Funding

The work was supported by the National Institutes of Health [grant numbers R37 AI34867 and R01 GM064625] to N.W.A. Deposited in PMC for release after 12 months.

#### References

- Andrews, N. W., Hong, K. S., Robbins, E. S. and Nussenzweig, V. (1987). Stage-specific surface antigens expressed during the morphogenesis of vertebrate forms of *Trypanosoma cruzi*. *Exp. Parasitol.* **64**, 474–484.
- Arantes, R. M. and Andrews, N. W. (2006). A role for synaptotagmin VII-regulated exocytosis of lysosomes in neurite outgrowth from primary sympathetic neurons. *J. Neurosci.* **26**, 4630–4637.
- Boyd, C., Hughes, T., Pypaert, M. and Novick, P. (2004). Vesicles carry most exocyst subunits to exocytic sites marked by the remaining two subunits, Sec3p and Exo70p. *J. Cell Biol.* **167**, 889–901.
- Fernandes, M. C., Cortez, M., Flannery, A. R., Tam, C., Mortara, R. A. and Andrews, N. W. (2011). *Trypanosoma cruzi* subverts the sphingomyelinase-mediated plasma membrane repair pathway for cell invasion. *J. Exp. Med.* **208**, 909–921.
- Guo, W., Grant, A. and Novick, P. (1999). Exo84p is an exocyst protein essential for secretion. *J. Biol. Chem.* **274**, 23558–23564.
- Guo, W., Sacher, M., Barrowman, J., Ferro-Novick, S. and Novick, P. (2000). Protein complexes in transport vesicle targeting. *Trends Cell Biol.* **10**, 251–255.
- He, B. and Guo, W. (2009). The exocyst complex in polarized exocytosis. *Curr. Opin. Cell Biol.* **21**, 537–542.
- He, B., Xi, F., Zhang, J., TerBush, D., Zhang, X. and Guo, W. (2007). Exo70p mediates the secretion of specific exocytic vesicles at early stages of the cell cycle for polarized cell growth. *J. Cell Biol.* **176**, 771–777.
- Heider, M. R. and Munson, M. (2012). Exorcising the exocyst complex. *Traffic* **13**, 898–907.
- Hsu, S. C., TerBush, D., Abraham, M. and Guo, W. (2004). The exocyst complex in polarized exocytosis. *Int. Rev. Cytol.* **233**, 243–265.
- Idone, V., Tam, C., Goss, J. W., Toomre, D., Pypaert, M. and Andrews, N. W. (2008). Repair of injured plasma membrane by rapid Ca<sup>2+</sup>-dependent endocytosis. *J. Cell Biol.* **180**, 905–914.
- Liu, J. and Guo, W. (2012). The exocyst complex in exocytosis and cell migration. *Protoplasma* **249**, 587–597.
- Liu, J., Zuo, X., Yue, P. and Guo, W. (2007). Phosphatidylinositol 4,5-bisphosphate mediates the targeting of the exocyst to the plasma membrane for exocytosis in mammalian cells. *Mol. Biol. Cell* **18**, 4483–4492.
- Liu, J., Yue, P., Artym, V. V., Mueller, S. C. and Guo, W. (2009). The role of the exocyst in matrix metalloproteinase secretion and actin dynamics during tumor cell invadopodia formation. *Mol. Biol. Cell* **20**, 3763–3771.
- Liu, J., Zhao, Y., Sun, Y., He, B., Yang, C., Svitkina, T., Goldman, Y. E. and Guo, W. (2012). Exo70 stimulates the Arp2/3 complex for lamellipodia formation and directional cell migration. *Curr. Biol.* **22**, 1510–1515.
- Martinez-Arca, S., Alberts, P., Zahraoui, A., Louvard, D. and Galli, T. (2000). Role of tetanus neurotoxin insensitive vesicle-associated membrane protein (TI-VAMP) in vesicular transport mediating neurite outgrowth. *J. Cell Biol.* **149**, 889–900.
- Moskalenko, S., Tong, C., Rosse, C., Mirey, G., Formstecher, E., Daviet, L., Camonis, J. and White, M. A. (2003). Ral GTPases regulate exocyst assembly through dual subunit interactions. *J. Biol. Chem.* **278**, 51743–51748.
- Murthy, M., Garza, D., Scheller, R. H. and Schwarz, T. L. (2003). Mutations in the exocyst component Sec5 disrupt neuronal membrane traffic, but neurotransmitter release persists. *Neuron* **37**, 433–447.
- Reddy, A., Caler, E. V. and Andrews, N. W. (2001). Plasma membrane repair is mediated by Ca<sup>2+</sup>-regulated exocytosis of lysosomes. *Cell* **106**, 157–169.
- Rodríguez, A., Webster, P., Ortego, J. and Andrews, N. W. (1997). Lysosomes behave as Ca<sup>2+</sup>-regulated exocytic vesicles in fibroblasts and epithelial cells. *J. Cell Biol.* **137**, 93–104.
- Tam, C., Idone, V., Devlin, C., Fernandes, M. C., Flannery, A., He, X., Schuchman, E., Tabas, I. and Andrews, N. W. (2010). Exocytosis of acid sphingomyelinase by wounded cells promotes endocytosis and plasma membrane repair. *J. Cell Biol.* **189**, 1027–1038.
- Tardieux, I., Webster, P., Ravesloot, J., Boron, W., Lunn, J. A., Heuser, J. E. and Andrews, N. W. (1992). Lysosome recruitment and fusion are early events required for trypanosome invasion of mammalian cells. *Cell* **71**, 1117–1130.
- TerBush, D. R. and Novick, P. (1995). Sec6, Sec8, and Sec15 are components of a multisubunit complex which localizes to small bud tips in *Saccharomyces cerevisiae*. *J. Cell Biol.* **130**, 299–312.
- TerBush, D. R., Maurice, T., Roth, D. and Novick, P. (1996). The Exocyst is a multiprotein complex required for exocytosis in *Saccharomyces cerevisiae*. *EMBO J.* **15**, 6483–6494.
- Toomre, D., Steyer, J. A., Keller, P., Almers, W. and Simons, K. (2000). Fusion of constitutive membrane traffic with the cell surface observed by evanescent wave microscopy. *J. Cell Biol.* **149**, 33–40.
- Tweten, R. K. (2005). Cholesterol-dependent cytolysins, a family of versatile pore-forming toxins. *Infect. Immun.* **73**, 6199–6209.
- Woolsey, A. M., Sunwoo, L., Petersen, C. A., Brachmann, S. M., Cantley, L. C. and Burleigh, B. A. (2003). Novel PI 3-kinase-dependent mechanisms of trypanosome invasion and vacuole maturation. *J. Cell Sci.* **116**, 3611–3622.
- Zuo, X., Zhang, J., Zhang, Y., Hsu, S. C., Zhou, D. and Guo, W. (2006). Exo70 interacts with the Arp2/3 complex and regulates cell migration. *Nat. Cell Biol.* **8**, 1383–1388.